AAS 19-265

A TITAN GRAVITY-ASSIST TECHNIQUE FOR BALLISTIC TOURS SKIMMING OVER THE RINGS OF SATURN

Mar Vaquero[*], Juan Senent[†], and Matthew Tiscareno[‡]

A novel type of Titan-flyby orbits featuring passes of the Saturn rings at close range has been recently discovered. The purpose of this study is to explore the trajectory design space and assess the applicability of such orbits to the design of a Saturn Ring Tour mission concept. A set of initial conditions required to start a tour of the rings is first determined and a flyby sequence to maximize the science observation time over desired ring regions in terms of range distance, relative velocity and duration is then selected. To demonstrate the potential of this technique, a sample high-fidelity ballistic ring tour is detailed.

BACKGROUND AND MOTIVATION

Saturn's main rings consist of billions of mostly water-ice particles, ranging from microscopic to many meters in diameter and moving in quasi-circular orbits around Saturn with orbit radii from 67,000 to 137,000 km.[1] The main rings are divided into four regions, A through D, as shown in Figure 1; the F and G rings, at larger radii, are more tenuous but yet of great scientific interest. Many questions are still unanswered regarding the rings formation and the microphysical interactions between particles in Saturn's rings. Within their own Keplerian motion, ring particles can bend, spin, and collide individually, or collectively form density waves and gaps that gather particles into long, thin structures that then dissolve back into new separate particles.[2] The character and behavior of these particles is not only a topic of scientific interest in planetary ring dynamics, but also a crucial component in the understanding of the dynamics and time scales of planetary accretion disks that build planets around stars.[3] Moreover, there is still no consensus as to the ring particles' mechanism of formation; some features of the rings suggest a relatively recent origin, but certain models indicate they are much older and likely to have formed early in the Solar System's history.[4]

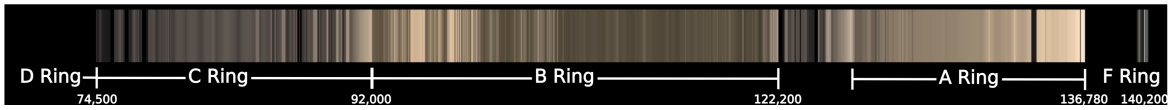

Figure 1. Natural-color mosaic of Saturn's main rings, A through D, along with more tenuous F ring. (Images taken by Cassini narrow-angle camera on May 9, 2007.)

Thus far, there have not been any direct, high resolution observations of individual ring particles. For decades, scientists have been interested in a trajectory that would enable close-up passes of the

[*]Mission Design Engineer, NASA Jet Propulsion Laboratory, California Institute of Technology, Pasadena, CA
[†]Engineering Applications Software Engineer, NASA Jet Propulsion Laboratory, California Institute of Technology
[‡]Carl Sagan Center for the Study of Life in the Universe, SETI Institute, Mountain View, CA
Pre-decisional information, for planning and discussion only.

rings of Saturn to provide the observations needed to constrain and discriminate among dynamical models. Previous Cassini studies made a number of simplifying assumptions that would disable the use of Titan flybys for ring-skimming trajectories.[5] As an alternative to a flyby-powered trajectory, the 2012 Planetary Science Decadal Survey (PSDS) Giant Planets Panel (GPP) commissioned a JPL-led Technology Trade Study to examine the technological feasibility for a Saturn Ring Observer (SRO) mission concept. The goal of this mission was to carry out in situ studies of Saturn's rings from a spacecraft placed in a circular orbit a few kilometers above the ring plane.[6] The two primary objectives specified by the GPP were to 1) investigate the method(s) by which a spacecraft might be placed and maintained in a hover orbit at Saturn and 2) identify technological developments for the next decade that would enable such a mission in the post-2023 time frame. The Study Questionnaire also called out power, propulsion, and trajectory technologies as the highest priorities. The selected team of experts proposed a continuous low-thrust ion engine to maintain the vertical displacement of the spacecraft over the ring plane and chemical thrusters to allow it to "hop" over vertical obstacles in the rings, such as bending waves and out-of-plane ringlets.[6] Among some of the technical challenges encountered during the study was the direct insertion into the hover orbit from Saturn approach, which involved a ΔV of 10 km/s, forcing the use of nuclear electric propulsion and guided aerocapture techniques at Titan.[7] It was concluded that, although quite promising, extensive new technology was required and the concept maturity level was low.

During a previous alternate end-of-mission study for Cassini, a novel type of flyby orbits featuring passes within 200 km of the Saturn rings was discovered.[8] By exploiting Titan gravity assists, such orbits require no ΔV (ballistic in nature) nor new technology development. In fact, this type of trajectory, illustrated in Figure 2, could have been flown by Cassini in March 2016. Note that this trajectory features one short ring-skimming pass leading to a Saturn impact orbit. In this paper, the theoretical aspects and orbital geometries that enable the proposed ring-skimming trajectory are detailed. The trajectory design space is explored and a range of suitable initial conditions needed to start a tour of the rings are determined, followed by the flyby sequence required to study different ring regions. A graphical approach is proposed to aid the trajectory designer in determining a sequence to cover different radii of the ring plane (inside/outside) to maximize the science return. To demonstrate the potential of this concept, a sample high-fidelity tour covering different ring regions in terms of range distance, relative velocity, and duration is illustrated.

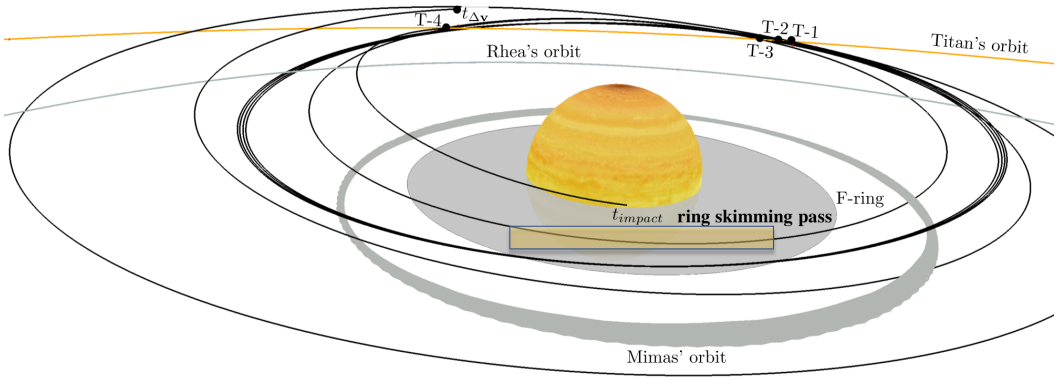

Figure 2. Four Titan-flyby trajectory featuring one ring-skimming pass and ending on impact with Saturn, plotted in a Saturn-centered inertial frame. (Graph from Vaquero and Senent[8])

THE RINGS AS OBSERVED BY CASSINI

During its Grand Finale, Cassini flew repeatedly through the gap between Saturn and its inner most ring;[9,10] throughout this series of 22 fast, highly inclined (62 degrees), short period (6.5 days) orbits, Cassini recorded valuable data to enable the scientific community to better understand Saturn's complex ring system. Even though the spacecraft did not fly close to the rings during the tour, it collected valuable images immediately before and after the Saturn Orbit Insertion (SOI) burn on July 1, 2004; less than 2 hrs before its closest approach to Saturn, the spacecraft first crossed through the large gap between the F ring and G ring, at a distance of roughly 158,500 km from the planet's center.[11] During the SOI burn, which lasted 96 min, Cassini passed behind the following regions as seen from Earth: 1) F ring at SOI + 23 min, 2) A ring at SOI + 30 min, C) Cassini division at SOI + 55 min, B ring at SOI + 1 hr 01 min, and C ring at SOI + 1 hr and 18 min. Unfortunately, there was no science data recorded during the SOI burn time period (illustrated by the shaded region in Figure 3). After the SOI burn was completed, Cassini coasted above the rings of Saturn for approximately one hour and 44 minutes before it descended back through the ring plane.[12] Invaluable scientific data was recorded during this short time frame. Used as a reference in this study, the trajectory appears plotted in blue in Figure 3. The left vertical axis curve (black) on the bottom plot represents the relative altitude of Cassini with respect to the ring plane, and the right vertical axis curve (red) shows the relative velocity also with respect to the ring plane, as a function of time.

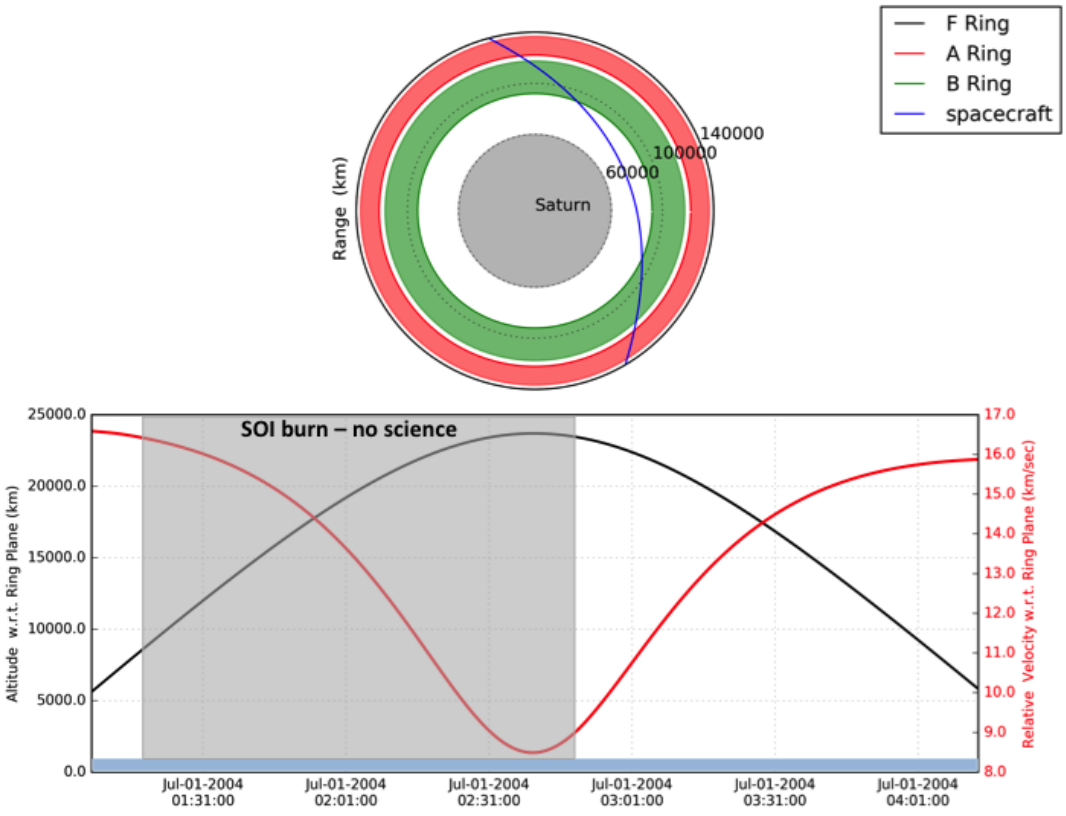

Figure 3. Polar plot (top) illustrating Cassini's trajectory passing over the rings of Saturn during the SOI burn. The bottom plot shows the corresponding altitude over the ring plane in black and the spacecraft relative velocity in red.

At periapsis, with a relative tangential velocity of 8.5 km/s, Cassini flew over the ring plane at an altitude of 25,000 km; however, no data was collected at closest approach. The proposed ring-skimming technique results in passes at much closer ranges and slightly lower relative velocities, which would improve tremendously the resolution of any images taken of ring particles. For reference, the light blue shaded region at the bottom of the polar plot in Figure 3 represents the altitude range covered by a sample ring-skimming orbit with closest approach below 1,000 km.

RINGS SCIENTIFIC INTEREST: GOALS, OBJECTIVES AND INSTRUMENTATION

There are many unanswered questions regarding the rings and inner moons of Saturn. By exploiting the proposed ring-skimming technique, scientists could potentially find answers to questions like, did a catastrophic event occur in the Saturn system 100 million years ago? did the inner moons form from rings, or are the rings a product of a breakup of inner moons? As part of this study, and to understand the full potential of such a mission concept, a team of ring scientists gathered to explore the possibilities. The highlights below are a brief summary of the ring science goals and objectives that Tiscareno, Hedman, and Estrada defined for a Saturn ring-skimming mission concept:[13]

Study disk processes, using the rings as a natural laboratory, to understand particle interactions and the origins and operations of disk-embedded objects. Understanding the individual and collective interactions of continuum ring particles could be done by measuring both the velocity dispersion of these particles and the dynamics of collisions between two individual ring particles. A camera with 10cm resolution and sufficient spatial and temporal coverage to see mutual particle motion and a collision would be sufficient to observe these phenomena. Additionally, the vertical structure and/or layering of ring particles could be analyzed by adding stereo imaging. Lastly, understanding the origins and operations of disk-embedded objects, such as propellers in the A ring and the moonlets causing "fans" and "jets" in the F ring, could be accomplished by imaging and occultations.

Study system origin and history, using the rings as a tracer. The composition of ring particles, giving chemical clues to Saturn system origins, could be analyzed by measuring the color reflectance of individual ring particles and textures at various locations in the rings, with the same camera and possibly with passive radiometry. A dust detector could enable the measurement of the chemical composition of particles recently ejected from the ring plane at various locations. Additionally, measuring dynamical properties of particles within and above the rings and characterizing the frequency, properties, and evolution of impact ejecta could help scientists understand the transport processes within rings.

Study processes in the Saturn environment, using rings as a detector. Observations of impact ejecta clouds, down to small sizes and in large numbers, would characterize the population of heliocentric objects entering the Saturn system. Searching for seismological structures in the rings would characterize the internal structure of Saturn.

With these objectives in mind, a ballistic, high-fidelity ring-skimming tour was generated following the design process described in the following sections.

ANALYTICAL DERIVATION OF RING-SKIMMING ORBITAL EXPRESSIONS

A theoretical study was carried out to provide a set of basic orbital elements to construct a conic trajectory to skim over the rings satisfying some geometric conditions. The derivation of the relevant expressions is detailed in this section.

Parametrization of ring-skimming orbital geometries

The orbital elements that define a ring-skimming trajectory can be determined by four quantities – k_1, k_2, k_3 and k_4 – associated with the geometry of a ring pass, as depicted in Figure 4. These four quantities are defined as follows,

k_1, k_2 Radii of the first and second ring crossings, respectively: $k_1, k_2 > 140180$ km, which corresponds to the maximum F ring radius (points A and C in Figure 4).

k_3 Magnitude of the projected spacecraft position vector at the maximum altitude over the rings (point B in Figure 4).
[66900 km (min. D ring radius) $\leq k_3 \leq$ 140180 km (max. F ring radius)]

k_4 Maximum altitude (signed) over the rings (point B in Figure 4). By convention, a negative sign is used for passes below the ring plane.

r_{max} Spacecraft radius at the maximum altitude over the rings, i.e., $r_{max} = \sqrt{k_3^2 + k_4^2}$

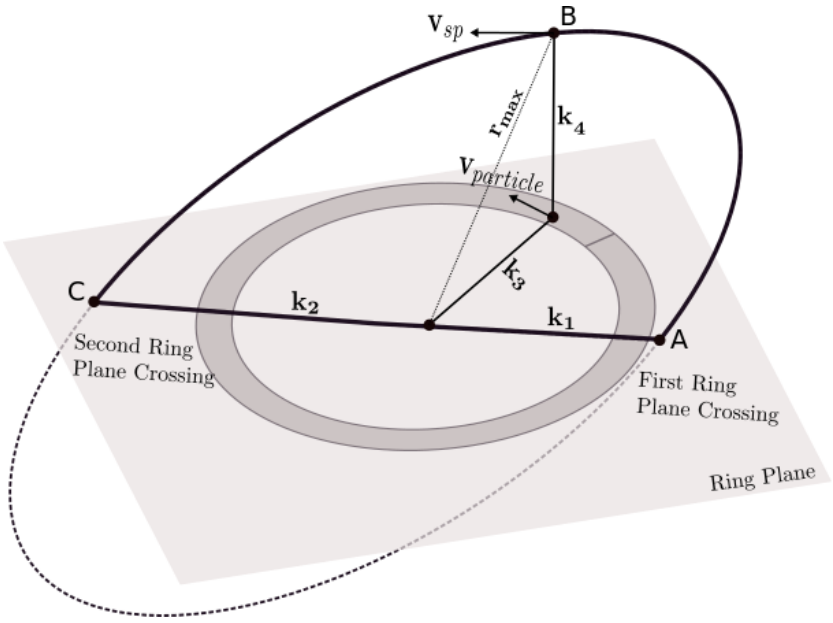

Figure 4. Geometry of the Saturn ring pass. $\mathbf{v}_{sp}$ is the velocity of the spacecraft and $\mathbf{v}_{particle}$ is the velocity of a ring particle associated with the spacecraft position.

In general, the node crossings (k_1 and k_2) should be located outside the overall ring disk, i.e., the node crossings must be outside of the F ring radius. Although not considered in this investigation, it is possible to find ring-skimming trajectories with nodes located at one of the ring gaps, such as the Cassini Division. The location over the rings where the maximum altitude is achieved (k_3 and k_4) is defined next. If the node distances are equal, that is, $k_1 = k_2$, then the relative radial velocity between the spacecraft and a ring particle located directly underneath the spacecraft is zero and the relative tangential velocity is at its maximum, as illustrated in Figures 3 and 10. The true anomaly at the points A, C and B in Figure 4 is given by,

$$f_1 = -\omega,\ f_2 = \pi - \omega,\ f_{max} \tag{1}$$

where ω is the argument of periapsis. The true anomaly of the orbit at point B is then derived from the following two equations,

$$\dot{z} = \sqrt{\frac{\mu}{p}}\left[(\cos f + e)\sin i\cos\omega - \sin\theta\sin i\sin\omega\right] = 0 \tag{2}$$

$$\cos\left(\omega + f_{max}\right) = -e\cos\omega \tag{3}$$

where e and i represent orbital eccentricity and inclination, respectively. The set of orbital elements is then determined by solving a system of equations. First, the equation for the position magnitude is rewritten as,

$$r = \frac{p}{1 + e\cos\left(\theta - \omega\right)} \text{ where } \theta = \omega + f \tag{4}$$

The application of a change of variable,

$$P = e\cos\omega,\ \ Q = e\sin\omega \tag{5}$$

yields three equations,

$$\begin{array}{lll} \frac{p}{k_1} - P\cos\theta_1 - Q\sin\theta_1 = 1 & & \theta_1 = 0 \\ \frac{p}{k_2} - P\cos\theta_2 - Q\sin\theta_2 = 1 & \text{where} & \theta_2 = \pi \\ \frac{p}{r_{max}} - P\cos\theta_3 - Q\sin\theta_3 = 1 & & \theta_3 = \omega + f_{max} \end{array} \tag{6}$$

$$\begin{aligned} \frac{p}{k_1} - P &= 1 \\ \frac{p}{k_2} + P &= 1 \\ \frac{p}{r_{max}} - P\cos\theta_3 - Q\sin\theta_3 &= 1 \end{aligned}$$

The semilatus rectum of the orbit, p and P, are obtained from the first two equations,

$$p = \frac{2}{\left(\frac{1}{k_1} + \frac{1}{k_2}\right)} = \frac{2k_1k_2}{k_1 + k_2} \tag{7}$$

$$P = \frac{p}{2}\left(\frac{1}{k_1} - \frac{1}{k_2}\right) = \frac{k_2 - k_1}{k_1 + k_2} \tag{8}$$

Note that neither p nor P depend on k_3 or k_4. When $k_1 = k_2$ (as it was in the case of Cassini during SOI, Figure 3), the maximum altitude is obtained at periapsis. That is,

$$P = 0 \rightarrow P = e\cos\omega = 0 \rightarrow e = 0, \text{ or } \omega = \frac{\pi}{2}, \frac{3\pi}{2} \tag{9}$$

$$\sin\theta_3 = \text{sgn}\left(k_4\right) = \text{sgn}(Q) \rightarrow \begin{cases} if\, k_4 > 0 \rightarrow \omega = \frac{\pi}{2} \rightarrow f_{max} = 0 \\ if\, k_4 < 0 \rightarrow \omega = -\frac{\pi}{2} \rightarrow f_{max} = 0 \end{cases} \tag{10}$$

The rest of the orbital elements are then obtained from Eq. 3,

$$\cos\theta_3 = -e\cos\omega = -P \tag{11}$$

and an expression for $\sin\theta_3$ is obtained by solving for prograde orbits, i.e., $\sin i > 0$,

$$k_4 = r_{max}\sin\left(\omega + f_{max}\right)\sin i \rightarrow \text{sgn}\, k_4 = \text{sgn}\left[\sin\left(\omega + f_{max}\right)\right] = \text{sgn}\left(\sin\theta_3\right) \tag{12}$$

$$\sin\theta_3 = \text{sgn}\left(k_4\right)\sqrt{1 - P^2} \text{ and } Q = \frac{-1 + \frac{p}{r_{max}} + P^2}{\sin\theta_3} \tag{13}$$

The set of relevant orbital elements is given by,

$$\begin{aligned} \omega &= atan2\left(Q,\, P\right) \\ e &= \sqrt{P^2 + Q^2} \\ i &= \arcsin\left(\frac{k_4}{r_{max}\sin\theta_3}\right) \\ a &= \frac{p}{1 - e^2} \end{aligned} \tag{14}$$

where a represents the semi-major axis. The right-ascension of the ascending node, Ω, does not depend on the geometrical parameters of the ring pass. Therefore, Ω is a free parameter that can be used to target the appropriate Titan flyby. In a patched-conic sense, the plane of the orbit must contain Titan's position vector at the flyby and as such, there are two solutions for Ω.

Characterization of ring-skimming enabling Titan flybys

To characterize the conditions of Titan flybys that support ring-skimming passes, it is necessary to make certain simplifying assumptions: 1) Titan moves on a circular orbit around Saturn, 2) the node crossing radii of the ring-skimming trajectories (k_1 and k_2) are equal, and 3) in general, $k_3 \gg k_4$. For different types of ring-skimming passes, the flyby v_∞ is given by the following expression,[14]

$$v_\infty = v_b\sqrt{3 - \frac{r_b}{a} - 2\sqrt{\frac{p}{r_b}}\cos i} \tag{15}$$

where r_b and v_b represent the position and velocity magnitudes of the flyby body. In this investigation, trajectories exploiting only Titan flybys are presented, but the technique was successfully applied to other bodies, such as Rhea. The $\cos i$ term can be eliminated from the expression above by considering the second simplifying assumption. That is, from Eq.14 and when $k_1 = k_2 \rightarrow P = 0 \rightarrow \sin\theta_3 = \text{sgn}\,(k_4)$, and thus,

$$\cos i = \cos\left(\arcsin\left(\frac{|k_4|}{r_{max}}\right)\right) = \sqrt{1 - \frac{k_4^2}{r_{max}^2}} = \frac{k_3}{\sqrt{k_3^2 + k_4^2}} \approx 1 \tag{16}$$

The semi-major axis, a, depends only on the pump angle of the flyby.[15] Therefore, for a given v_∞, the parameter p of the orbit is obtained using Eq. 15 and the parameter k_3 can be computed as follows,

$$r_{max} = \frac{p}{1 + \sqrt{1 - p/a}} \rightarrow k_3 = \sqrt{r_{max}^2 - k_4^2} \tag{17}$$

The families of ballistic ring-skimming tours can be characterized by defining two parameters at the Titan flyby: v_∞ and pump angle (or equivalently, an orbit resonance). To illustrate this process, the solution space for ring-skimming ballistic tours for a set of v_∞ magnitudes and orbit resonances is shown in Figure 5. The different curves on this plot represent the range of radii that can be covered given a range of v_∞ magnitudes. In fact, given certain conditions, all of the main rings of Saturn (that is, D ring through F ring) can be covered without the need of any deterministic maneuvers. For instance, values close to $V_\infty \approx 6$ km/s yield passes over rings at 6 different k_3 ranges: D-ring(1), C-ring(3), B-ring(1) and F-ring(1) with maximum relative tangential velocities between $[6.2,\ 8.9]$ km/s.

Relationship between relative velocity and maximum altitude over the rings

For ring-skimming enabling Titan flybys to exist, the orbital inclination is restricted to be close to that of Titan's orbit. Consequently, the maximum altitude over the rings (i.e., k_4) is also constrained. However, this restriction does not affect the range of attained relative velocities with respect to ring particles. To demonstrate this, Figure 6 illustrates the geometry of a ring-skimming pass for a selected fixed resonance and v_∞ at Titan when the maximum altitude over rings is varied. In this particular example, the resulting ring-skimming pass provides coverage of the D ring and it was selected because it is representative of the worst-case scenario in terms of relative velocity variation. As it can be seen in Figure 6, the duration of the passes (at different altitudes) is close to 20 minutes and the relative tangential and radial velocities are essentially the same for all the selected altitude values. To observe larger variations, the maximum altitude would have to be increased to 23,700 km (similar to Cassini's altitude during the SOI burn pass over the rings). However, at this altitude, the orbital inclination would also significantly increase, eliminating the possibility of exploiting Titan flybys for ring-skimming trajectories.

Characterization of the maximum relative tangential velocities with respect to ring particles

Following the second simplifying assumption, when the node crossing distances are equal ($k_1 = k_2$), the relative tangential velocities with respect to the ring particles achieve their maximum value at maximum altitude over the rings, as illustrated in Figure 6. At this point in the orbit, the relative

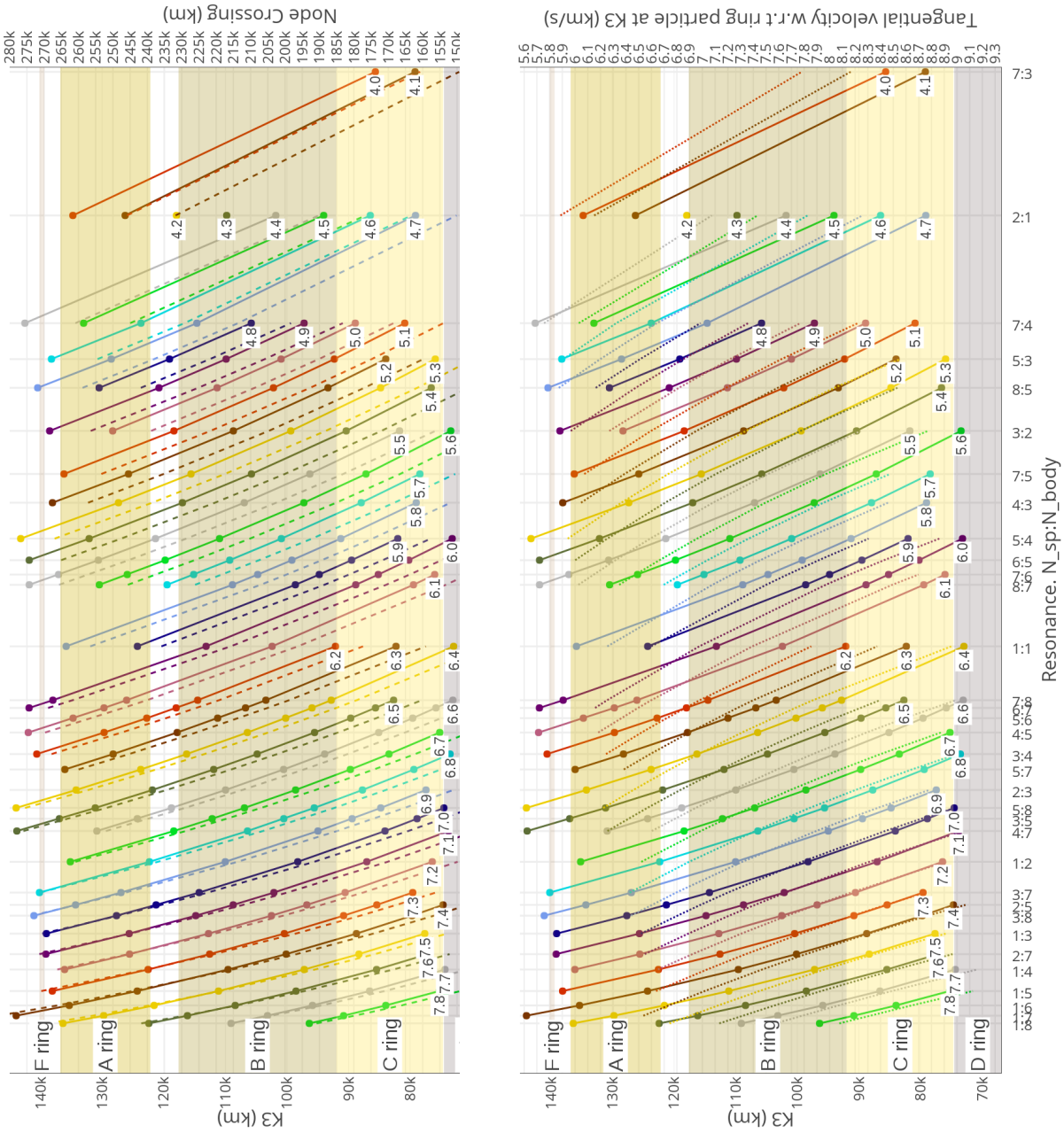

Figure 5. Ballistic ring-skimming tour space for families of Titan flybys. Each family corresponds to a level of v_∞ at Titan. The relationship between the ring distance (solid line) and node location (dashed line) is shown in the left figure. The right figure shows the relationship between the ring distance (solid line) and the relative tangential velocity between the spacecraft and a ring particle (dashed line) at the maximum altitude over the rings.

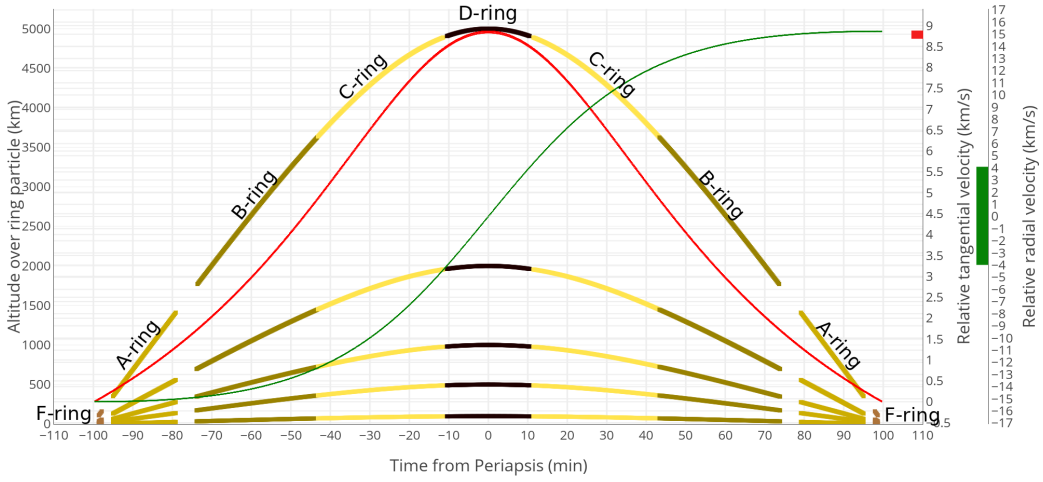

Figure 6. Ring pass duration and relative tangential and radial velocities as a function of maximum altitude over the rings (k_4) variation.

radial velocities with respect to the particles located on the projection of the spacecraft position vector are zero, as demonstrated in Figure 6. This location on the orbit can then be used to characterize the relative velocities with respect to the ring particles. Given that the inclination of the ring-skimming trajectories is close to zero, the spacecraft tangential velocity (v_T) can be approximated as the velocity at periapsis (v_p),

$$v_T \approx v_p = \sqrt{\frac{\mu}{r_{particle}}\left(\frac{2a - r_{particle}}{a}\right)} \tag{18}$$

Assuming that the ring particles move in circular orbits on the plane of Saturn's equator, the maximum relative tangential velocity can be computed as,

$$v_T - v_{particle} = \sqrt{\frac{\mu}{r_{particle}}\left(\frac{2a - r_{particle}}{a}\right)} - \sqrt{\frac{\mu}{r_{particle}}} = \sqrt{\frac{\mu}{r_{particle}}}\left(\sqrt{2 - \frac{r_{particle}}{a}} - 1\right) \tag{19}$$

The maximum relative tangential velocities over different ring locations are shown in Figure 7. Two types of flybys are considered: Titan (red) and Rhea (green). In general, Rhea flybys provide lower relative tangential velocities. However, the pumpdown sequence from SOI to the beginning of a ring-skimming tour requires more ΔV.

A SAMPLE RING-SKIMMING TOUR

To characterize and better understand the nature of gravity-assist trajectories to support a potential future mission to observe the rings of Saturn at close range, a sample ballistic tour was designed. In the span of only 162 days and without using any propellant, this sample tours covers the main ring regions in 13 low-altitude passes. To further demonstrate the feasibility of the concept, a high-

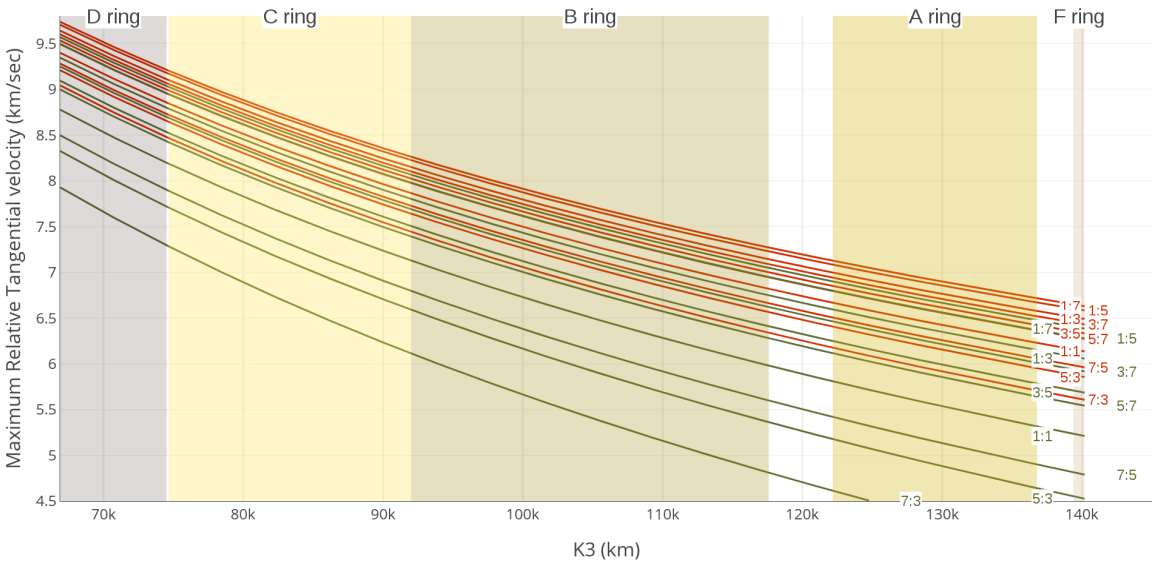

Figure 7. Maximum relative tangential velocity for Titan (red) and Rhea (green) flybys for different orbit resonances and ring particle locations. For visual clarity, not all the available resonances are shown.

fidelity transfer trajectory from Earth was designed and connected to the tour and several spacecraft disposal options were evaluated, including impact orbits with Saturn and Tethys.

Earth to Saturn: interplanetary cruise, capture, and pumpdown phases

The sample tour generated in this study follows an interplanetary trajectory from Earth to Saturn with a nominal launch date of February 25, 2025. The 8.5 year long cruise baseline is a Venus-Earth-Earth gravity-assist (VEEGA) trajectory with an initial C3 departure value of 17.65 km^2/s^2 and a deep space maneuver (DSM) of 13.04 m/s in between the two Earth flybys. Note that a 21-day launch period analysis was carried out resulting in a departure C3 range between 16 to 18.75 km^2/s^2.[16] In addition, a backup launch opportunity was identified in July 2026 with a very low C3 (9 km^2/s^2) and Saturn arrival in 2034. It is important to note that every trajectory presented in this investigation is calculated in a full ephemeris model. For illustration purposes, the baseline cruise trajectory is represented in Figure 8.

After arriving at Saturn on January 4, 2034 with a v_∞ of 6.75 km/s, the corresponding SOI burn (ΔV = 646.8 m/s) is performed to place the spacecraft into a 180-day capture orbit around Saturn with an inclination of 15.8 deg with respect to the ring plane. A Periapsis Raising Maneuver (PRM) with a magnitude of 381.2 m/s is then performed to target the first Titan flyby with a v_∞ of 5.14 km/s. The total ΔV for the capture phase of the mission is 1,028 m/s and the time-of-flight (TOF) is 9.34 years. The resulting capture trajectory appears in the center plot in Figure 8. Once captured around Saturn, the pumpdown sequence begins to reduce the orbital inclination all the way down to the ring plane ($i < 0.40$ deg). A feasible (but certainly not unique) sequence that requires no maneuvering and approximately 5-months is shown in the right plot (Figure 8).[17] For completeness, the main trajectory events from launch to the end of the pumpdown sequence are detailed in Table 1.

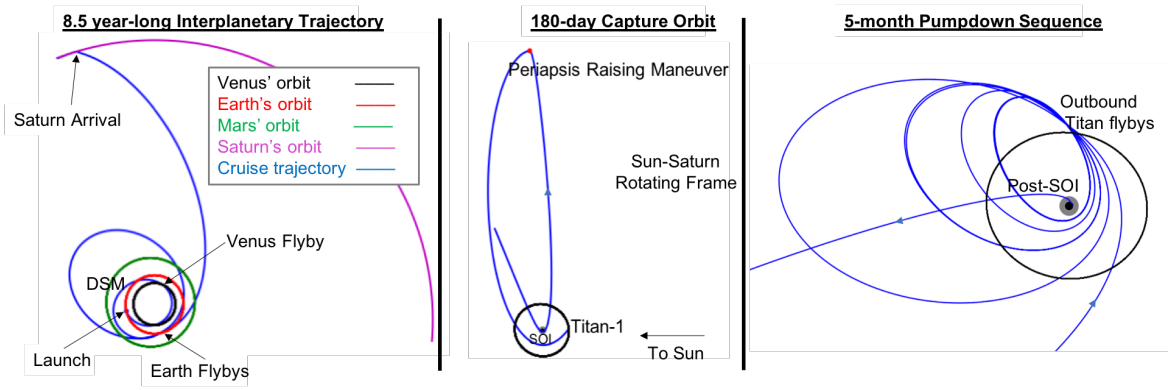

Figure 8. Transfer trajectory analysis from Earth to Saturn: interplanetary cruise (left, plotted in a Sun-centered inertial frame), capture orbit (center, plotted in a Sun-Saturn rotating frame) and pumpdown sequence (right, plotted in a Saturn-centered inertial frame).

Ring-skimming phase

Once the spacecraft reaches the equatorial plane, the ring-skimming phase begins. A sample Saturn rings tour is represented in Figure 10, featuring 13 passes over the rings (but below the ring plane) over 162 days. The scientific objective of this tour is to enable ring studies for satellite and ring formation and evolution (waves, propellers). In particular, there are three regions that are of scientific interest:

D Ring: periapsis range $<$ 75,000 km

C Ring: 75,000 km $<$ periapsis range $<$ 92,000 km

B Ring: 92,000 km $<$ periapsis range $<$ 122,200 km

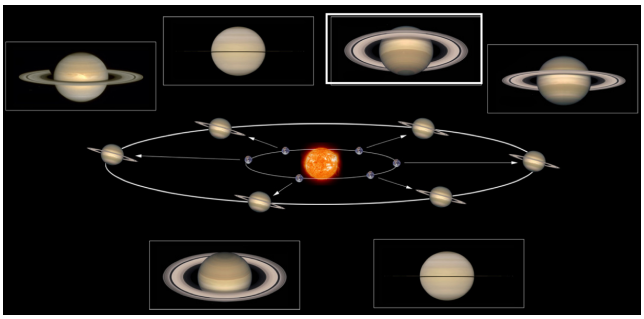

Figure 9. The changing aspect of Saturn's Rings.[18]

Particle observations must occur on the sunlit side of the rings, that is, the rings must be observed when the ring opening angle to the Sun is less than the maximum ring slope. The images in Figure 9 (courtesy of ©thChieh2008[18]), show how Saturn looks like from Earth as both Earth and Saturn orbit around the Sun. For reference, Saturn competes a full orbit around the Sun in the same time that Earth makes 29.457 revolutions. For the selected time frame of this mission, Saturn's orientation is highlighted in the white boxed image in the upper right corner of Figure 9. Hence, in order for the observations to occur on sunlit side, the passes over the rings must occur "below" the ring plane (i.e., altitude $<$ 0 km).

The sample ballistic 162-day tour exploits 3 targeted and one untargeted Titan flybys to attain the desired geometry over the rings and features multiple non-targeted flybys of the smaller moons, including Enceladus, Dione, Rhea, and Mimas. Each orbit presents low relative velocity passes over the rings, ranging from 1.5 to 3.0 hours in length, with an orbital period of 10-14 days. The

Table 1. Burns and flybys from Earth to Saturn's ring plane

Event	Epoch	Flyby Altitude	
Earth Departure	25-FEB-2025	180 km	C3 = 17.65 km^2/s^2
Venus Flyby	23-AUG-2025	7103 km	$v_\infty v_\infty$ = 8.93 km/s
Earth Flyby	05-JUL-2026	433 km	v_∞ = 11.12 km/s
Deep Space Maneuver	25-FEB-2028	–	ΔV = 13.04 m/s
Earth Flyby	05-JUL-2029	293 km	v_∞ = 11.07 km/s
Saturn Arrival	04-JAN-2034	3900 km	v_∞ = 6.75 km/s
Saturn Orbit Insertion	04-JAN-2034	–	ΔV = 646.8 m/s
Periapsis Raising Maneuver	30-MAR-2034	–	ΔV = 381.2 m/s
Titan - 1 Flyby	27-JUN-2034	1000 km	v_∞ = 5.14 km/s
Titan - 2 Flyby	14-AUG-2034	1000 km	v_∞ = 5.14 km/s
Titan - 3 Flyby	30-SEP-2034	999 km	v_∞ = 5.14 km/s
Titan - 4 Flyby	16-OCT-2034	1946 km	v_∞ = 5.14 km/s
Titan - 5 Flyby	02-DEC-2034	6970 km	v_∞ = 5.14 km/s

maximum orbital inclination is 0.55 degrees with respect to the ring plane, resulting in multiple near equatorial passes over the three desired regions ranging in altitude from 1,000 km to 6 km. The plots in Figure 10 highlight some of the characteristics of this tour. The color represents the passes over the rings grouped by Titan flyby, e.g., red corresponds to the orbits between the 6th and 7th Titan flybys, green between the 7th and 8th flybys, yellow corresponds to the passes between Titan-8 and Titan-9, and lastly, blue indicates the last passes after Titan-9 on April 8, 2035. The bottom plots represent altitude with respect to the ring plane (left) and relative velocity (right), split into radial and tangential components. Three particular bands were selected for the design of this tour but, overall, this new technique enables the design of flyby trajectories that drastically improve the coverage of most of the rings region while using no ΔV. Further insight can be gained by examining the osculating orbital elements associated with these ring-skimming orbits. The graphs in Figure 11 illustrate the evolution of the orbital period, inclination, and periapsis range as a function of time. For reference, the epoch associated with each Titan flyby is marked by a vertical, colored, solid line: red (Titan-6), green (Titan-7), yellow (Titan-8), and blue (Titan-9).

The design process for this ring-skimming tour began with the v_∞ and geometry conditions from the last Titan flyby in the pumpdown phase and the graph in Figure 5. After an initial guess for the tour was generated, a corrections scheme was used to re-converge the trajectory in the full ephemeris model while preserving the characteristics of the ring passes. Figure 12 illustrates how well the converged trajectory (green curve) compares to the initial guess (patched-conics). It is important to note that the v_∞ magnitudes reported in Figure 12 are patched-conic values and two of the transfers along the converged trajectory are non-resonant flyby arcs. The red curve corresponds to a flyby v_∞ of 5.6 km/s and the dark green line represents the geometry achieved with a v_∞ of 5.65 km/s. It is clear how the full ephemeris trajectory "bounces" between both curves.

A wide range of possible altitudes and relative velocities can be attained using the proposed technique. While the altitudes are generally quite low, the velocity, especially the tangential component, is on the higher end of the desired values, ranging from 5.6 km/s in the F ring to 9.1 km/s in the D ring. Nevertheless, these relatively high tangential velocities are not an issue for scientific observations if the instrument is placed on a scanning platform and a strategy is implemented to mitigate any possible smearing.

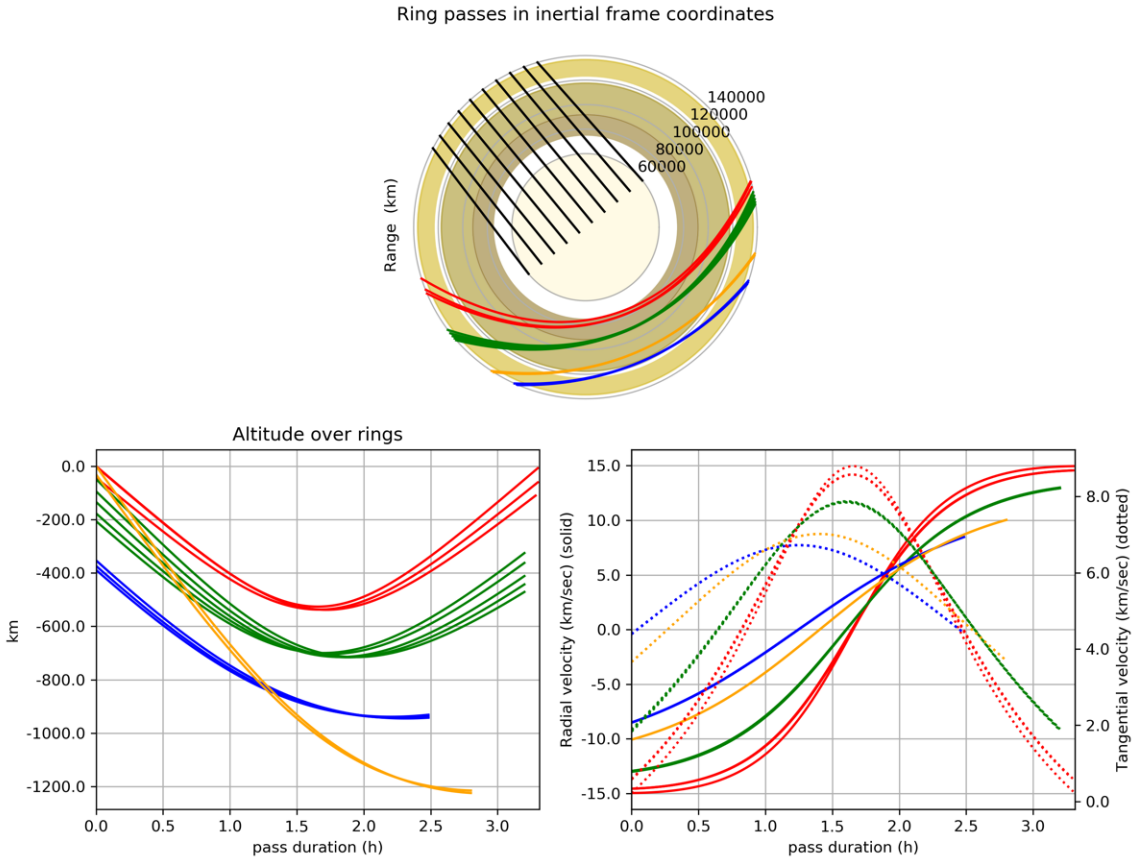

Figure 10. Polar plot (top) illustrating 13 passes over the rings of Saturn corresponding to the 162-day long sample ballistic tour; the altitude and relative velocity curves (bottom) represent the passes over the B, C, and D rings. The black solid lines on the top plot represent the region of the rings shadowed by the Sun and, thus, in eclipse. This ring-skimming trajectory is ballistic ($\Delta V = 0$ m/s) and exploits four Titan gravity assists. For reference, the ring passes are color coded and grouped by Titan flybys.

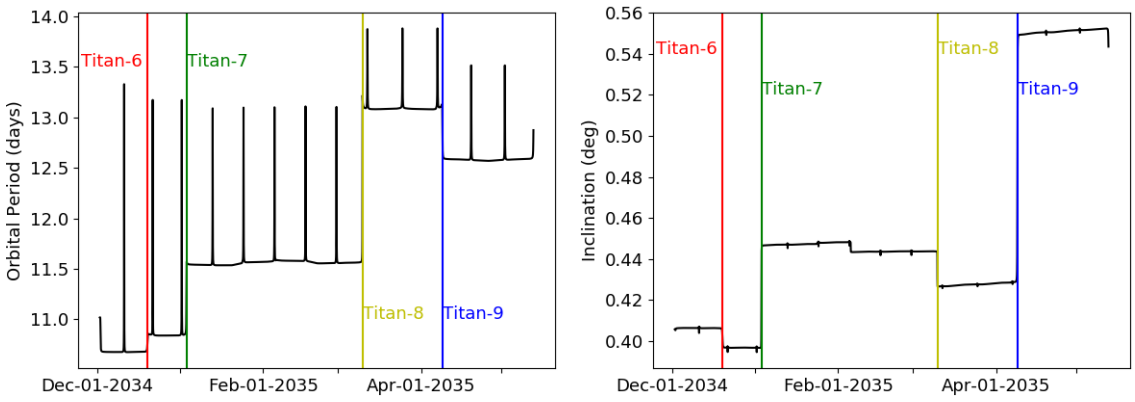

(a) Osculating period in days

(b) Osculating inclination in degrees

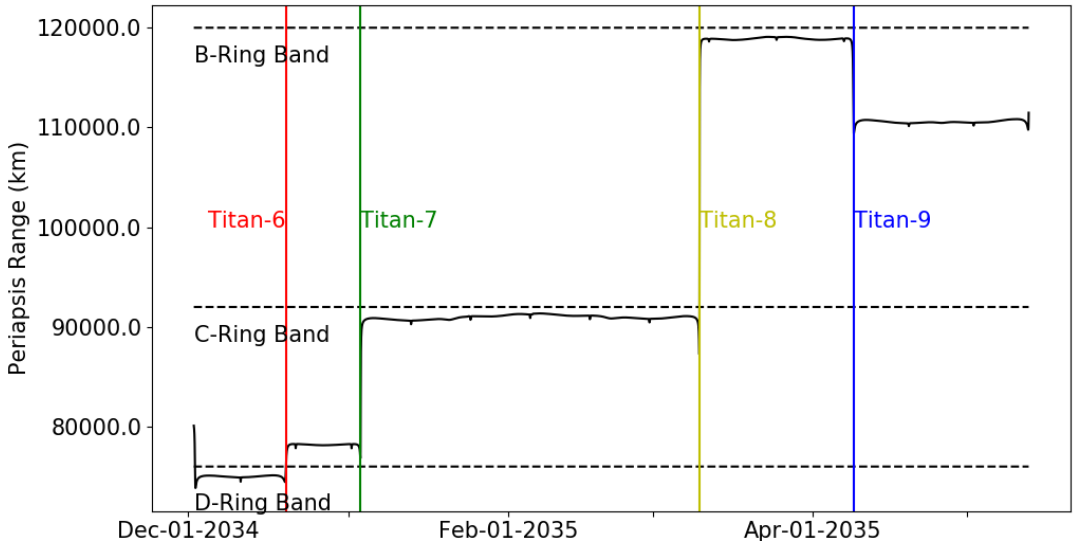

(c) Osculating periapsis range in km

Figure 11. Osculating orbital elements associated with the sample ring-skimming trajectory depicted in Figure 10, grouped by Titan flyby.

Tour engine: targeted Titan flybys

Much like Cassini's trajectory design, the changes necessary to attain the desired ring geometries are accomplished using Titan gravity assists. For this mission concept study, the assumed total propellant at launch is enough to alter the spacecraft's velocity by about 1,700 m/s. However, more than half of this ΔV is already used by the time the spacecraft reaches the ring plane. As a general reference, a single flyby of Titan at an altitude of 1,000 km provides a change in velocity of about 800 m/s. Therefore, just like Cassini did, the ring-skimming spacecraft takes advantage of Titan's gravity to explore different ring regions. Details about the four Titan flybys that enable the geometry depicted in Figure 10 are listed in Table 2.

Titan's thick atmosphere imposes a minimum flyby constraint of 1,000 km. Based on Cassini navigation experience, thermal and attitude control considerations due to the atmospheric drag are the limiting factors. Unlike the flybys in the pumpdown phase, the Titan flybys in the ring-skimming phase occur at rather high-altitudes and are, therefore, not a challenge from a navigation perspec-

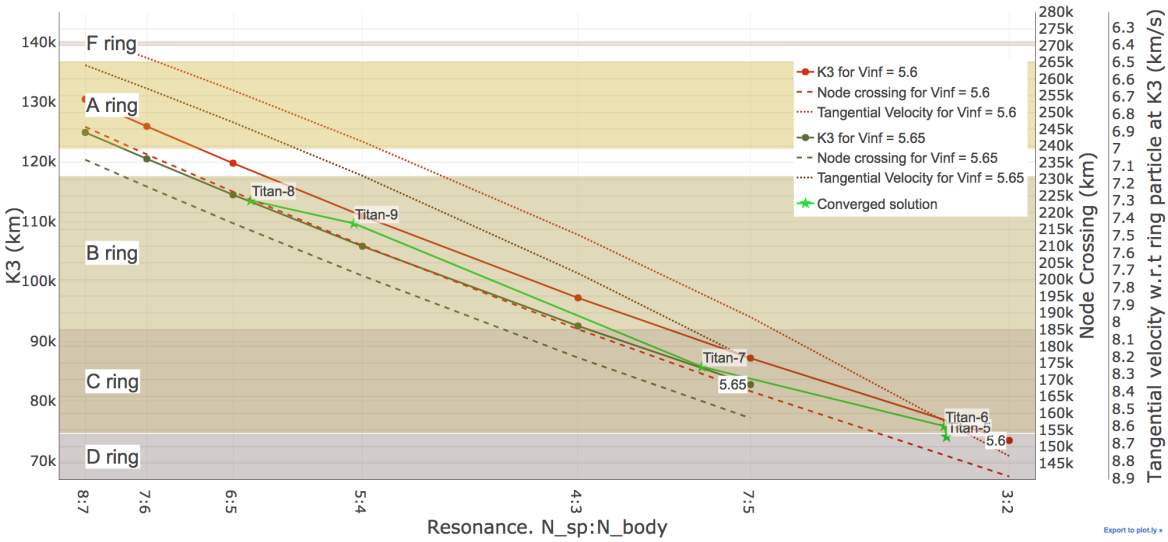

Figure 12. K3 (left vertical axis), and node crossing distance and velocity (right vertical axis) as a function of the resonant ratio (horizontal axis), defined as N_{sc}:N_{body}, for the initial patched conic guesses (red and dark green curves) and the converged tour in the ephemeris model (light green curve).

Table 2. Targeted Titan flybys that enable the ballistic ring-skimming sequence

Flyby	Epoch	Flyby Altitude	v_∞	Color Code
Titan-6	19-DEC-2034	56,882 km	5.30 km/s	red
Titan-7	03-JAN-2035	15,039 km	5.53 km/s	green
Titan-8	10-MAR-2035	6,222 km	5.49 km/s	yellow
Titan-9	08-APR-2035	28,036 km	5.29 km/s	blue

tive. Additional constraints are also considered in the design of these targeted flybys, such as the minimum time between encounters. The time in between flybys must be long enough to allow time for tracking and the incorporation of statistical maneuvers before and after every flyby to accurately navigate the tour. For the sample tour in Figure 10, the shortest time span in between flybys is 15 days, which is plenty to meet general navigation and spacecraft operations requirements.

Bonus science: untargeted Icy Moons flybys

One of the key aspects to the ring-skimming technique is to maintain the trajectory inclination with respect to the ring plane as low as possible, while keeping the ascending and descending nodes outside of the F ring to protect the spacecraft from potential ring particle impacts. Most of the smaller, inner moons orbit in the same plane as the rings, with tiny orbital inclinations with respect to Saturn's equatorial plane: Enceladus (0.004 deg), Mimas (1.58 deg), Dione (0.032 deg), and Rhea (0.32 deg). For comparison purposes, Figure 11(b) illustrates the near equatorial orbital inclination of the ring-skimming tour as a function of time. Because of this orbital geometry, there are multiple untargeted flybys of the inner moons that could be of much scientific interest. In particular, during

the sample ring-skimming tour, there are five untargeted flybys of Mimas, four of Enceladus, one of Dione, and three flybys of Rhea. The flyby epoch, altitude, and v_∞ corresponding to each of these untargeted flybys is listed in Table 3. With the appropriate instrument, distant flyby imaging of Mimas, Dione and Enceladus can be achieved when the spacecraft passes within 100,000 km of the target. Additionally, distant plume imaging of Enceladus could be done from as far as 200,000 km.[19] The corresponding icy moons groundtracks appear in Figures 13–14. Most of these tracks occur at low-latitudes over the northern and southern moon hemispheres; however, with some design tweaks and the addition of small maneuvers, these flybys could be targeted to obtain the desired groundtracks to meet scientific requirements.

Table 3. Untargeted Icy Moon Flybys

Flyby	Epoch	Flyby Altitude	v_∞
Enceladus-1	21-DEC-2034	33,289 km	11.77 km/s
Mimas-1	01-JAN-2035	36,291 km	11.84 km/s
Dione-1	13-JAN-2035	69,368 km	13.15 km/s
Rhea-1	24-JAN-2035	25,373 km	9.31 km/s
Rhea-2	05-FEB-2035	16,306 km	9.99 km/s
Mimas-2	05-FEB-2035	43,698 km	10.24 km/s
Enceladus-2	16-FEB-2035	16,307 km	13.76 km/s
Mimas-3	16-FEB-2035	16,001 km	14.78 km/s
Enceladus-3	28-FEB-2035	56,950 km	15.97 km/s
Rhea-3	06-APR-2035	33,298 km	8.75 km/s
Mimas-4	19-APR-2035	94,976 km	19.38 km/s
Mimas-5	02-MAY-2035	21,328 km	13.44 km/s
Enceladus-4	02-MAY-2035	68,812 km	8.32 km/s

SIGNIFICANCE OF RESULTS

This new family of gravity assists trajectories could enable a Saturn ring-focused Discovery or New Frontiers class mission, providing several orders of magnitude improvement from the highest resolution ring images that Cassini obtained in 2004 and with a much simplified mission architecture and operations schedule than the proposed ring hover mission concept. The uniqueness of the proposed concept resides in the fact that it does not require any new technology. In fact, a ring-skimming like trajectory could have been flown by Cassini in March, 2016. The proposed technique enables repeated passes – at least 4 per month – over the rings of Saturn for several hours each. By selecting the appropriate flyby sequence and orbital geometry, all regions of the main rings can be explored with minimal use of propellant. This is, indeed, another key feature of the ring-skimming technique; low, if not zero, ΔV requirement, which extends the mission length by multiple years. With only one or two instruments onboard the spacecraft (i.e., a camera and a dust detector) and the ability to fly so close to the ring plane, many questions regarding the formation, composition, structure, and interaction of ring particles could be answered. Moreover, the addition of the icy moons untargeted flybys may further enhance the scientific value of this Saturn System mission concept by also focusing on Titan, Enceladus, and and some of the other smaller moons.

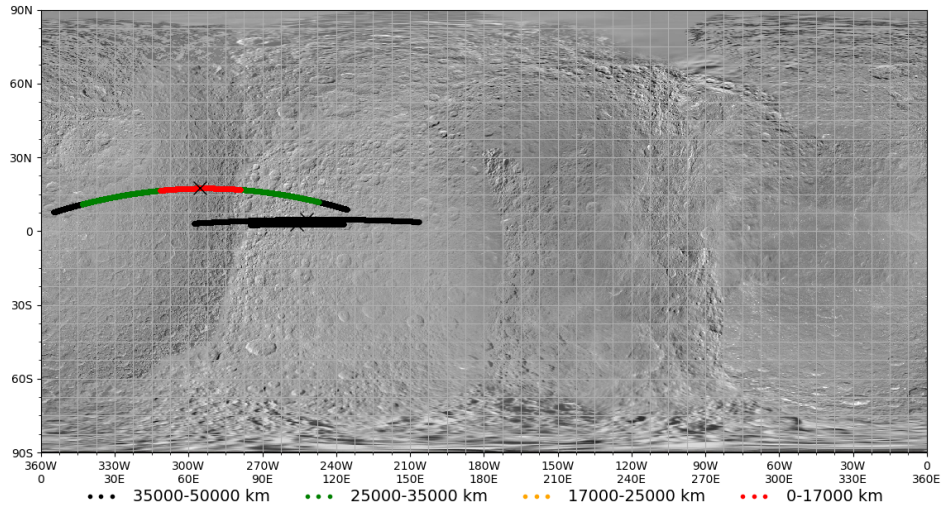

(a) Rhea nadir groundtracks

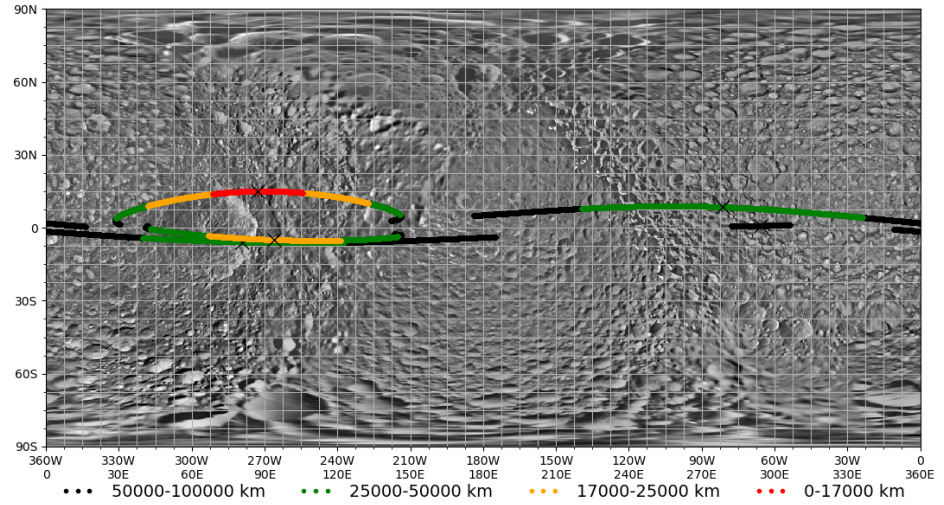

(b) Mimas nadir groundtracks

Figure 13. Rhea and Mimas nadir groundtracks corresponding to untargeted flybys during the ring-skimming phase. Closest approach is marked with an "x" and numbered in accordance with the flyby altitudes listed in Table 3.

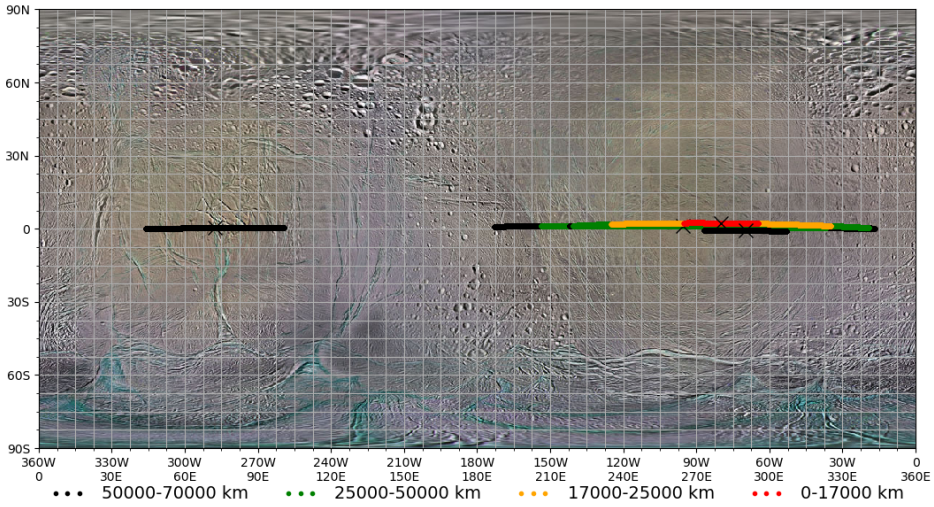

(a) Enceladus nadir groundtracks

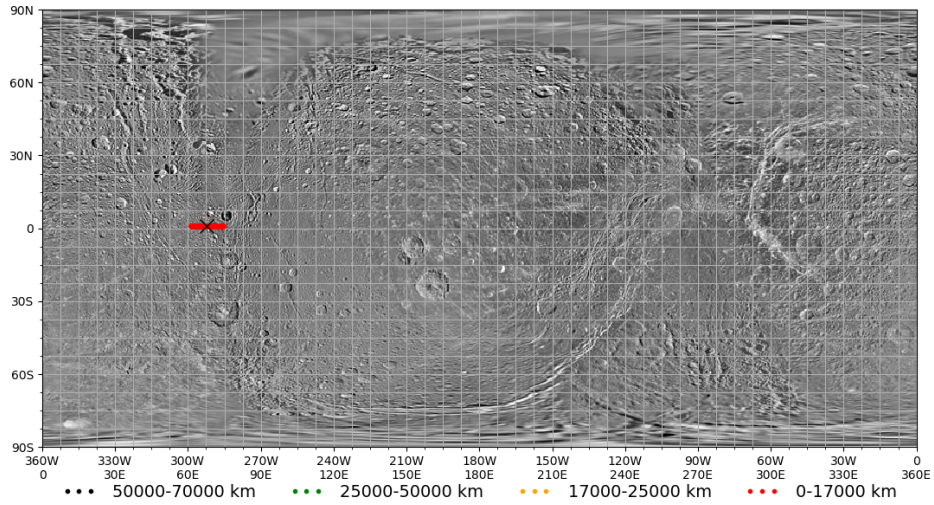

(b) Dione nadir groundtracks

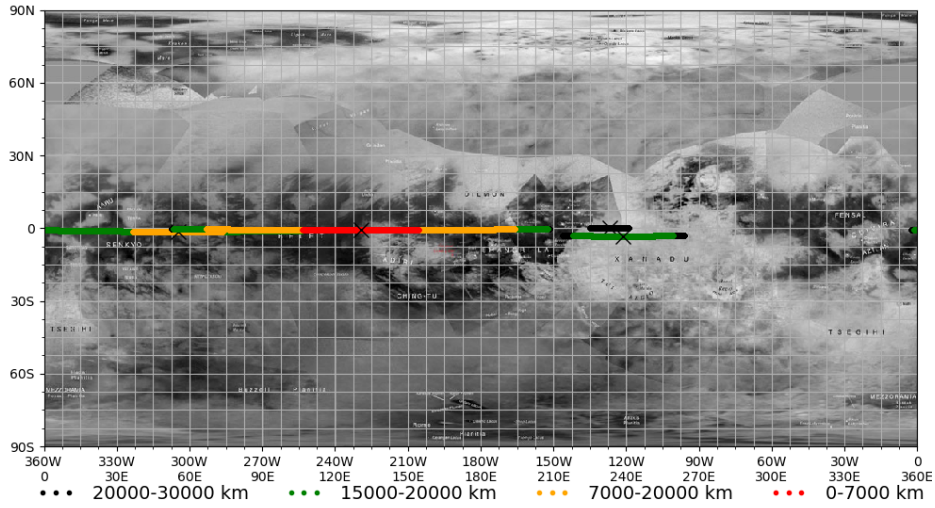

(c) Titan nadir groundtracks

Figure 14. Enceladus, Dione, and Titan nadir groundtracks corresponding to untargeted flybys during the ring-skimming phase. Closest approach is marked with an "x" and numbered in accordance with the flyby altitudes listed in Table 3.

ACKNOWLEDGMENT

The authors wish to acknowledge and thank Brent Sherwood (JPL Solar System Mission Formulation Office) and Nathan Strange (JPL Mission Systems Engineering Section), for their encouragement and support of this effort. Special thanks also go to ring scientists Matt Hedman (University of Idaho) and Paul Estrada (SETI Institute), who provided the scientific value to the proposed technique. Stefano Campagnola (JPL Mission Design and Navigation Section) also offered valuable insight into the graphical approach presented in this paper. This research was carried out at the Jet Propulsion Laboratory, California Institute of Technology, under a contract with the National Aeronautics and Space Administration. © 2019 California Institute of Technology. Government sponsorship acknowledged.

REFERENCES

[1] C. Porco, "Questions about Saturn's Rings," CICLOPS (Cassini Imaging Central Laboratory for Operations) , 2012.

[2] T. R. Spilker, "Saturn Ring Observer," *Acta Astronautica*, Vol. 52, 2003, pp. 259–265.

[3] M. S. Tiscareno and C. D. Murray, *Planetary Ring Systems. Properties, Structure, and Evolution*. Cambridge University Press, February 2018, doi: 10.1017/9781316286791.

[4] M. S. Tiscareno, *Planetary Rings*. Springer Science+Business Media Dordrecht: Planets, Stars and Stellar Systems, by T. Oswalt, L. French, and P. Kalas, Paul, 2013.

[5] C. H. Yam, D. C. Davis, J. M. Longuski, K. C. Howell, and B. Buffington,, "Saturn Impact Trajectories for Cassini End-Of-Mission," *Journal of Spacecraft and Rockets*, Vol. 46, March-April 2009.

[6] T. R. Spilker, "Saturn Ring Observer," *Forum on Innovative Approaches to Outer Planetary Exploration 2001-2020*, Jet Propulsion Laboratory, California Institute of Technology, Pasadena, California, Jan. 1, 2001.

[7] J. Casoliva and D. T. Lyons, "Mission Design of Guided Aero-Gravity Assist Trajectories at Titan," *AAS/AIAA Astrodynamics Specialist Conference*, Pittsburgh, Pennsylvania, August 9-13 2009. AAS Paper 09-432.

[8] M. Vaquero and J. Senent, "An Efficient Method to Design Premature End-Of-Life Trajectories: An Alternate Fate for Cassini," *25th International Symposium on Space Flight Dynamics*, Munich, Germany, October 19-23 2015.

[9] M. Wong, Y. Hahn, D. Roth, and M. Vaquero, "Trajectory Dispersion Control for the Cassini Grand Finale," *25th International Symposium on Space Flight Dynamics*, Munich, Germany., Oct. 19-23 2016.

[10] M. Vaquero, Y. Hahn, D. Roth, and M. Wong, "A Linear Analysis for the Flight Path Control of the Cassini Grand Finale Orbits," *26th International Symposium on Space Flight Dynamics*, Matsuyama, Japan, June 3-9 2017. ISTS-2017-d-010/ISSFD-2017-010.

[11] T. Goodson, B. Buffington, Y. Hahn, N. Strange, S. Wagner, and M. Wong, "Cassini-Huygens Maneuver Experience: Cruise and Arrival at Saturn," *AAS AIAA Astrodynamics Specialist Conference*, Lake Tahoe, California, August 7-11 2005. AIAA Paper 2014-4348.

[12] Cassini Mission, "Unlocking Saturn's Secrets: Cassini Saturn Orbit Insertion Timeline," nasa.gov, 2004.

[13] M. Tiscareno, M. Hedman, and P. Estrada, "Rings Science: Goals and Objectives," Internal Mission Concept Team Meeting, NASA Jet Propulsion Laboratory, Pasadena, California, January 22 2018.

[14] J. Miller and C. Weeks, "Application of Tisserand's Criterion to the Design of Gravity Assist Trajectories," *AIAA/AAS Astrodynamics Specialist Conference and Exhibit*, Monterey, California, August 5-8 2002. AIAA Paper 2002-4717.

[15] B. Buffington, N. Strange, and S. Campagnola, "Global Moon Coverage via Hyperbolic Flybys," *23rd International Symposium on Space Flight Dynamics*, Pasadena, California, Oct. 29 - Nov. 2 2012.

[16] J. Johannesen, "2025 Launch Period Analysis (CATO-based)," Internal Mission Design Team Meeting, NASA Jet Propulsion Laboratory, Pasadena, California, May 21 2018.

[17] S. Campagnola, "Tisserand Graph and V∞ Sphere," Internal Mission Design Team Meeting, NASA Jet Propulsion Laboratory, Pasadena, California, May 17 2018.

[18] My Dark Sky: Observations and Tips, "Ringless Saturn," mydarksky.org, March 26 2008.

[19] S. Lee, M. Hofstadter, M. Frerking, S. Gulkis, P. von Allmen, J. Crovisier, N. Biver, D. Bockelee-Morvan, L. Kamp, M. Choukroun, S. Keihm, and M. Janssen, "Sub-millimeter observation of water vapor at 557 GHz in Comet C/2002 T7 (LINEAR)," *Icarus*, Vol. 239, September 1 2014, pp. 141–453.